Conversion of single crystal mats to ultrahigh modulus polyethylene: the formation of a continuous crystalline phase

Jean M. Brady* and Edwin L. Thomas
Department of Polymer Science and Engineering, University of Massachusetts, Amherst, MA 01003, USA
(Received 11 May 1988; revised 16 January 1989; accepted 19 January 1989)

A series of ultrahigh modulus and strength polyethylene films of variable draw ratios (6–250), formed by the solid state coextrusion and post-drawing (SSE/PD) of single crystal mats, were analysed by transmission electron microscopy (TEM). The high performance mechanical properties of these materials were attributed to the formation of 'protofibrils'. Protofibrils are defined as long, highly crystalline fibrils which constitute a basic structural unit in ultradrawn polyethylene. The protofibrils observed here were made up of a series arrangement of ca. 8 nm thick 'kebabs' and crystalline 'bridges', were hundreds of nanometres long (along the chain direction), and were up to 10 nm wide. Darkfield TEM, which yields a lower bound of crystal size, revealed crystalline regions with a protofibril substructure which were at least 3 microns long. The observed evolution of morphology with draw suggested that protofibrils formed via a stress-induced rearrangement of the original single crystal mat morphology and subsequent strain-induced crystallization.

(Keywords: polyethylene; deformation; ultradrawn; shish kebabs; strain induced crystallization)

INTRODUCTION

It is now possible to generate highly crystalline polyethylene with a tensile modulus so high as to approach its theoretical crystalline phase modulus. This implies that under optimum drawing conditons, an exceedingly high degree of chain extension (e.g. large number of *trans* conformations in the chain) and subsequent strain-induced crystallization can be realized. For polyethylene, optimum drawing occurs at or above the alpha loss temperature, where crystal shear and chain slip are facilitated by a low yield stress, and chain scission is minimized[1,2].

Polyethylene can be ultradrawn in numerous ways. Conventional tensile drawing to very high draw ratios is often impractical, since materials tend to cavitate and undergo premature brittle failure[3]. Solid state extrusion (SSE) is an alternative method of uniaxial drawing. The major and perhaps most significant difference between SSE and tensile drawing is that SSE is accompanied by a high hydrostatic pressure. In both processes, the maximum achievable draw ratio increases with temperature, and similar draw ratios and tensile moduli can be attained, at least up to a draw ratio of one hundred[4]. At high draw ratios, the efficacy of tensile drawing is limited by the number density of entanglements and tie molecules. For instance, it has been shown that the tensile modulus reaches a plateau when HDPE of a molecular weight of (2×10^6) is drawn to a draw ratio of approximately 120 (ref. 5). Apparently, further drawing does not give rise to additional chain orientation, chain extension and strain-induced crystallization, or load bearing tie molecules.

The ultradrawing of polyethylene is accompanied by extensive molecular and morphological reorganization, as well as the associated changes in physical properties. Studies of changes in molecular mobility which accompany the drawing process using nuclear magnetic resonance (n.m.r.) have shown that noncrystalline phase chain mobility is inversely related to draw ratio. The mobility decreases sharply with increasing draw (at room temperature) to an extrusion draw ratio of ca. 12, and then gradually approaches a limiting value at higher draw ratios[6]. The sharp reduction in molecular mobility has been attributed to a high degree of chain orientation and extension within the amorphous phase. Upon reaching a draw ratio of ca. 10 (for room temperature drawing), initially spherulitic HDPE becomes fibrillar in appearance[7] and reaches its 'natural draw ratio'. Subsequent draw is accompanied by a rapid increase in draw stress, as well as an increase in crystallite size along the chain direction[6].

Other techniques provide an abundance of data which illuminate the deformation process. Density and infra-red measurements have revealed crystallinities as high as 90% in ultradrawn polyethylene[8,9]. Wide angle X-ray scattering has shown that crystals deform by $\langle 001 \rangle$ shear mechanisms during SSE. Crystallite dimensions along the a and b axes initially decrease and subsequently remain constant with draw[10–12]. Similar mechanisms operate during tensile drawing[13–15]. Crystal perfection, crystallinity, and crystallite dimensions along the c axis decrease and then increase with draw[3,11]. Calculations using Peterlin's morphological model[16] as well as scattering and density data have indicated that the number of crystalline bridges interconnecting lamellae increases with draw[11]. More importantly, the population of thick crystals plus crystalline bridges has been shown by darkfield TEM to increase with draw[17–20]. Indeed, a growing body of evidence supports the hypothesis that

* Present address, and to whom correspondence should be addressed: Mobil Chemical Company, PO Box 240, Edison, NJ 08818-0240, USA

0032-3861/89/091615-08$03.00

the morphology of ultradrawn polyethylene approaches one comprised of a sample spanning crystalline phase[8].

The concept of a continuous (sample spanning) crystalline phase was introduced long ago[21,22], although at the time the actual morphological data to support such a model was lacking. In a semicrystalline polymer such as polyethylene, the morphology could take the form of a composite with a crystalline matrix and an amorphous or defect rich 'filler' phase.

The drawing process which gives rise to high modulus polyethylene has been extensively studied not only by wide angle X-ray scattering (WAXS) but small angle X-ray scattering (SAXS) as well. It has been shown that the SAXS long period peak intensity decreases when polyethylene is drawn beyond a draw ratio of 10, and the fibrillar texture itself begins to deform[12,15]. In fact, ultradrawn polyethylene displays no long period reflections[9,23]. This indicates that the Peterlin and Gibson morphological models for drawn polyethylene, in which microfibrils consist of stacked lamellae which are interconnected by crystalline bridges, are not applicable to ultradrawn polyethylene.

The disappearance of SAXS intensity with draw has been interpreted in several ways. Scattering intensity is a function of both the mean squared electron density fluctuation between crystalline and amorphous phases as well as the ordering of those phases. If the densities of the amorphous and crystalline phases approach one another (while maintaining constant periodicity), scattering intensity drops. For polyethylene, the density of the amorphous phase is known to increase upon drawing, while the opposite is true for the crystalline phase[3,12]. However, it has been shown that the SAXS long period peak intensity of ultradrawn polyethylene does not increase when the sample is heated to melting, suggesting that density differences are not responsible for the loss of scattering intensity[9]. Alternatively, reductions in SAXS intensity can be attributed to variations in the volume fractions of the crystalline and amorphous phases[12]. It is also conceivable that the amorphous layers between lamellae elongate to different extents, due to local stress concentrations. This would give rise to more long period polydispersity, which would broaden the SAXS peak and reduce the maximum intensity of the long period reflection, as well as change the position of the peak depending on long period distribution[24]. Moreover, deformation can be so nonuniform as to obliterate any periodicity between amorphous and crystalline layers.

The multitude of explanations for the disappearance of a long period peak illustrates the fact that morphological models derived from scattering data are non-unique. Information gleaned from electron micrographs, however, provide the detailed information necessary to pinpoint the most plausible model. In the present studies, diffracting crystallites will be directly viewed (by darkfield TEM), elucidating the evolution of microstructure with draw.

EXPERIMENTAL

SSE/PD films were obtained from Dr T. Kanamoto for the present set of experiments. The SSE/PD process has been described elsewhere[1,8,25,26]. The specific samples used here were formed from single crystal mats of ultrahigh molecular weight polyethylene (UHMWPE, Hizex Million 240 M, $M_v = 1.5 \times 10^6$). These single crystals were grown under nitrogen for 20 h at 85°C from a 0.2% (w/w) xylene solution, containing 0.5% (w/w polymer) (2,6-di-t-butyl-*p*-cresol) as an anti-oxidant. The single crystal suspension was cooled to room temperature, filtered slowly, dried at room temperature, and then extracted with acetone, and dried for 20 h at 60°C. The mat was then solid state coextruded to a draw ratio of six at 110°C and subsequently uniaxially post-drawn at 125°C to total draw ratios as high as 250. Polyethylene drawn to draw ratios of 97 and 250 displayed tensile moduli exceeding 175 GPa and strengths exceeding 3 GPa[23].

For TEM studies, thin sections were removed from the bulk ultradrawn films using a detachment replication technique. First the fibres were etched in fuming nitric acid at ca. 80°C for 6 h. The films were then thoroughly rinsed in distilled water and subsequently dried in a vacuum oven. For detachment replication, several drops of a 5.0% (w/w) aqueous solution of polyacrylic acid (PAA, $M_w = 450\,000$) were placed on a glass slide. The glass slide had been cleaned and 'pretreated' with a thin coating of glycerol, facilitating the removal of PAA at a later stage. The etched polyethylene films were cut into very thin strips (ca. 1 mm wide) and laid on top of the wet PAA, taking care to make good surface contact.

After air-drying for at least 24 h, the polyethylene strips were removed from the PAA surface, and a thin carbon coating was evaporated onto the PAA surface. The areas of PAA where no polyethylene strips had been placed were then trimmed from the replica with a sharp razor blade. The areas potentially containing polyethylene remnants were scraped off the glass slide, cut into grid-sized pieces and floated onto the surface of distilled water, making sure that the PAA side was in contact with the water. The samples were left floating in water for at least 6 h. (Longer times are suggested.) The remaining carbon film and polyethylene remnants were then picked up from the water surface with copper grids, dried in a vacuum oven, and viewed by TEM.

The best TEM contrast was obtained in darkfield mode, as these materials were highly crystalline, and residual PAA could be excluded from the image. The (110), (200), (210), and (020) equatorial reflections were used. Observed crystal sizes must be considered as lower bounds, since slight bending out of the Bragg condition (by as little as 0.5 degrees), or the presence of defective crystalline regions (generated by nitric acid etching) could suggest the presence of a crystal boundary.

To ascertain that the observed morphology was not an artifact of nitric acid etching, samples which had not been exposed to nitric acid were observed. The conversion of lamellae to their mosaic block components and the deformation of these blocks led to a broad distribution of crystal thicknesses (*Figure 3b*). A comparison of *Figures 3a* and *3b* suggests that the population of small crystals may have been somewhat depleted by the nitric acid treatment. However, long crystalline regions can be seen in both cases.

RESULTS AND DISCUSSION

Our discussion addresses the evolution of crystalline phase morphology with SSE/PD for draw ratios ranging from 6 to 250. Special attention was given to the identification of those structural elements probably responsible for the ultrahigh modulus of these samples.

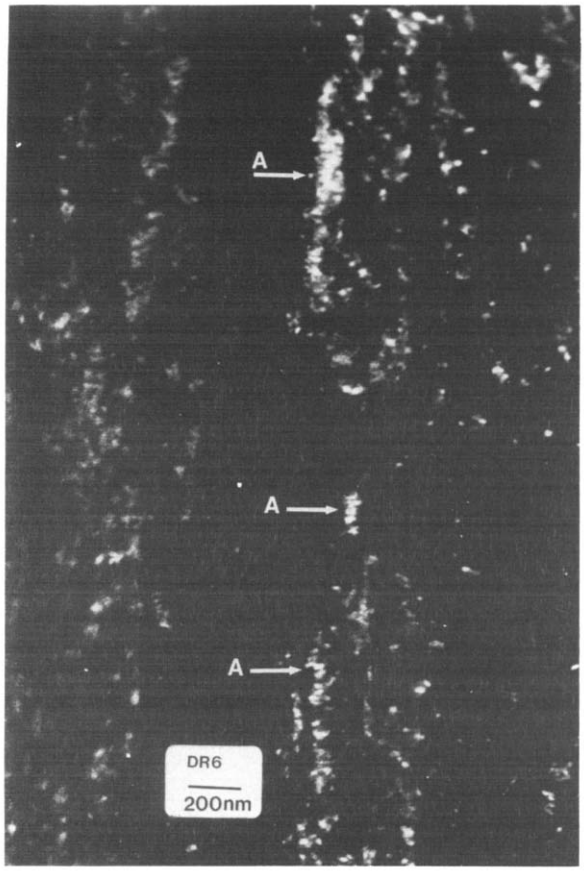

Figure 1 Darkfield micrograph of solid state extruded UHMWPE, draw ratio of 6, showing lamellar stacks. A mosaic block can be seen breaking away from the uppermost stack. Chain axis vertical in this and all subsequent figures

Solid state extrusion of UHMWPE single crystal mats to an extrusion draw ratio of 6 led to a morphology consisting of diffracting lamellae stacked along the chain direction (*Figure 1*, region A). Typically, the overall morphology was fibrous, and lamellae consisted of only a few laterally coalesced mosaic blocks. The mosaic blocks were ca. 20 nm thick (parallel to the chain axis) and wide. In some cases, thicker lamellae (ca. 37 nm) were seen (*Figure 2a*, region A), although mosaic blocks of 20 nm thickness were present nearby. The lamellae in *Figure 2* (regions A) appeared to be largely disrupted by the deformation, leaving behind numerous mosaic blocks with a wide distribution of sizes.

Polyethylene drawn to a draw ratio of 42 displayed large crystalline regions with a disrupted lamellar morphology and a mosaic block substructure (*Figure 3b*). This film appeared to be very fibrous. In *Figure 3a*, the conversion of lamellar stacks (region A), to a series of mosaic blocks (regions B) and subsequently to very highly crystalline fibrils, 'protofibrils', (regions C), was seen.

Protofibrils appear to be the fundamental structural units in ultradrawn polyethylene. In contrast to microfibrils, which display well defined alternating amorphous and crystalline layers, protofibrils appear to be structurally similar to needle crystals. Protofibrils have been shown to form by drawing microfibrils at elevated temperatures[27]. Close scrutiny of the protofibrils indicated that they were approximately 10 nm wide and were composed of a series arrangement of crystalline blocks of ca. 8 nm thickness. The protofibrils themselves were very highly oriented along the draw direction.

Much information can be gleaned about the drawing process by comparing morphologies which correspond to different draw ratios. At the early stages of drawing, single crystals apparently developed new grain boundaries, giving rise to a mosaic block substructure. At higher strains, the mosaic blocks sheared along the ⟨001⟩ direction, the defective regions between mosaic blocks (*Figure 2*), region B) being preferential sites of shear. The presence of lamellar stacks implied the presence of underlying needle crystals. Apparently, amorphous phase extension, orientation, and finally strain-induced crystallization led to needle crystal formation, the needle crystals acting as templates for lamellar overgrowth. Deformation and destruction of crystallites, followed by strain-induced (re)crystallization gave rise to the well known reduction and subsequent increase in average crystal thickness and crystallinity with draw.

The mechanisms by which the crystalline phase morphology was transformed during deformation have been detailed previously in thin film deformation studies[14,27,28]. Crystal shear and chain slip (chain unfolding and pullout) along the ⟨001⟩ direction reduce the lateral crystal width. Moreover, defective regions develop within crystallites, further reducing crystal thickness. Strain-induced crystallization assisted protofibril formation, as evidenced by the extensive (hundreds of nanometres) crystallographic registry within a

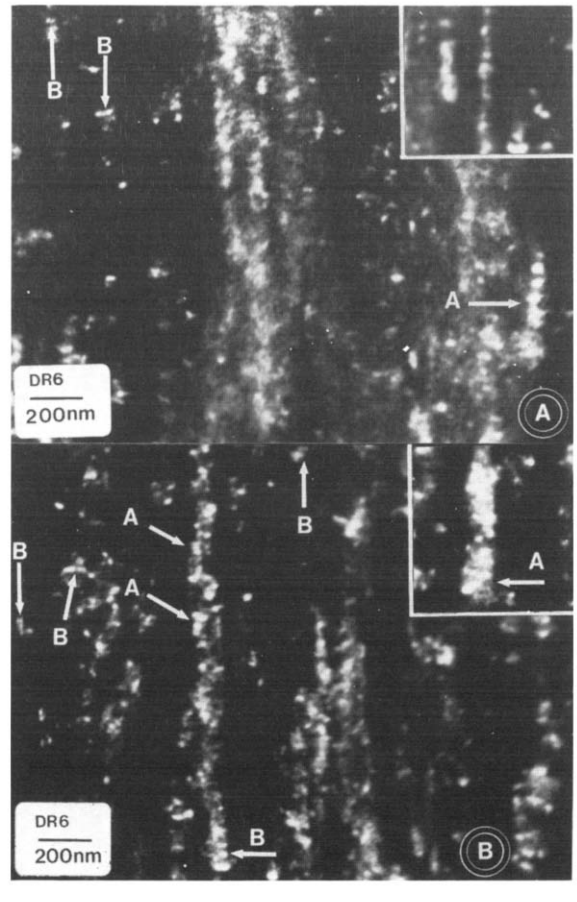

Figure 2 Darkfield micrograph of solid state extruded UHMWPE, draw ratio of 6, showing lamellar stacks (A) and defective regions between mosaic blocks (B)

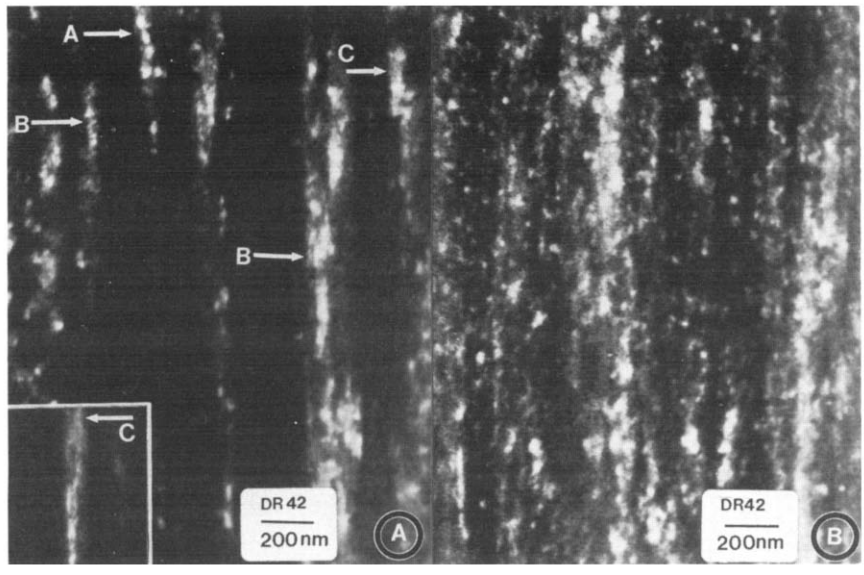

Figure 3 Darkfield micrograph of SSE/PD UHMWPE, draw ratio of 42, showing (a) lamellae interconnected by crystalline bridges (A), series of mosaic blocks (B), and protofibrils (C); and (b) microstructure of SSE/PD UHMWPE not exposed to nitric acid

protofibril. The protofibril morphology resembles that of a shish-kebab composed of almost all shish core or needle crystal (*Figures 4* and *5*). Kebabs appear only slightly wider than the core. These similarities suggest that shish-kebabs which are formed during solid state deformation and tensile drawing undergo the same yielding, crystalline phase deformation, and strain-induced crystallization processes which bring about protofibril formation.

The formation of protofibrils in ultrahigh tensile modulus polyethylene is consistent with the Peterlin model of deformation[16]. Peterlin's model attributes the increase of tensile modulus with draw ratio at high strains to an increase in the number of taut tie molecules, which in turn are formed by decreasing microfibril diameter through shear and chain slip. In the present case, such shear processes led to protofibril formation.

At a draw ratio of 97, crystalline bridges interconnecting long crystalline regions were visible (*Figure 6*, region A). Protofibrils up to hundreds of nanometres long had formed (*Figure 6*, region B). The diameter of an individual protofibril was often variable along its length. This is consistent with the mechanism of protofibril formation in which lamellae are converted to mosaic blocks which undergo further deformation (*Figure 7*, region A). Occasionally, the protofibrils appeared to laterally coalesce, forming wider crystalline regions (*Figure 7a*, region B).

The apparent protofibril coalescence implied that the thick crystalline regions shown in *Figure 7b* (region B) were composed of protofibrils. This was in contrast to material drawn to a draw ratio of 6, where crystalline regions were composed of lamellae (interconnected by crystalline bridges) of greater width (perpendicular to the chain direction) than thickness (parallel to the chain direction). Here, the lamellae themselves had been transformed into needle-like crystals (protofibrils), which were long along the chain direction but not very wide.

Observations at a draw ratio of 250 substantiated the formation of protofibrils (*Figures 8* and *9*, region A), as well as the generation of large crystalline regions (up to

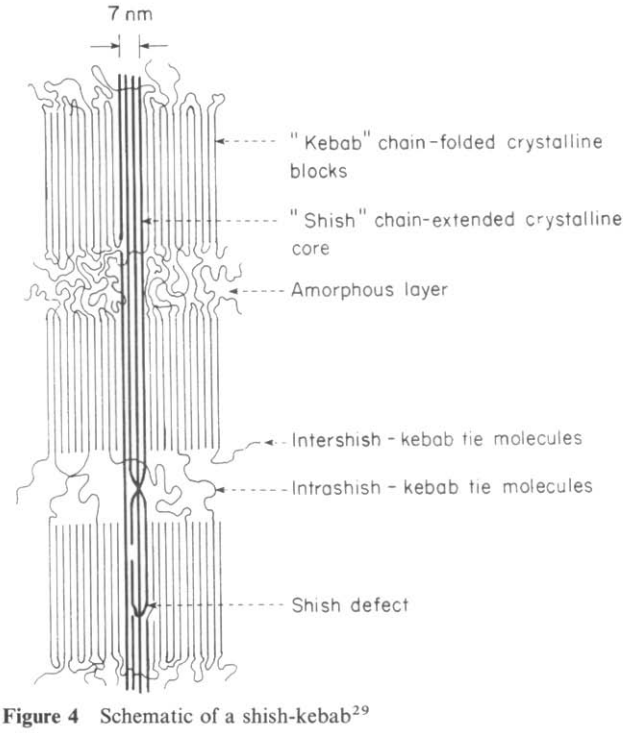

Figure 4 Schematic of a shish-kebab[29]

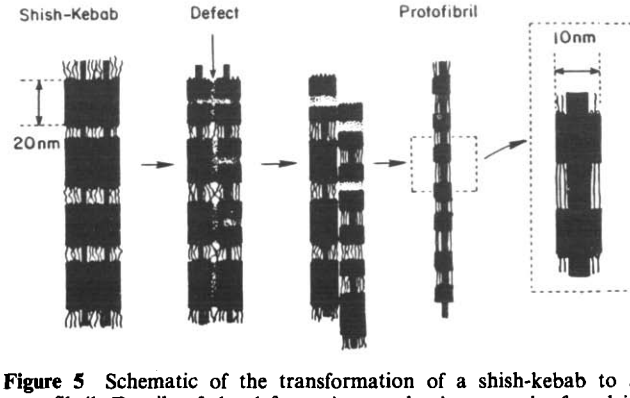

Figure 5 Schematic of the transformation of a shish-kebab to a protofibril. Details of the deformation mechanisms can be found in previous publications[14,27]

3 microns long along the chain direction) similar to those seen in thin film deformation studies[27,28]. The large crystalline regions were composed of coalesced protofibrils rather than stacked lamellae (*Figures 8* and *9*, region B). In fact, at this draw ratio, no stacked lamellae were seen. This concurred with previous reports that the crystallite microstructure of ultradrawn polyethylene bore little resemblance to precursor morphology[30,31].

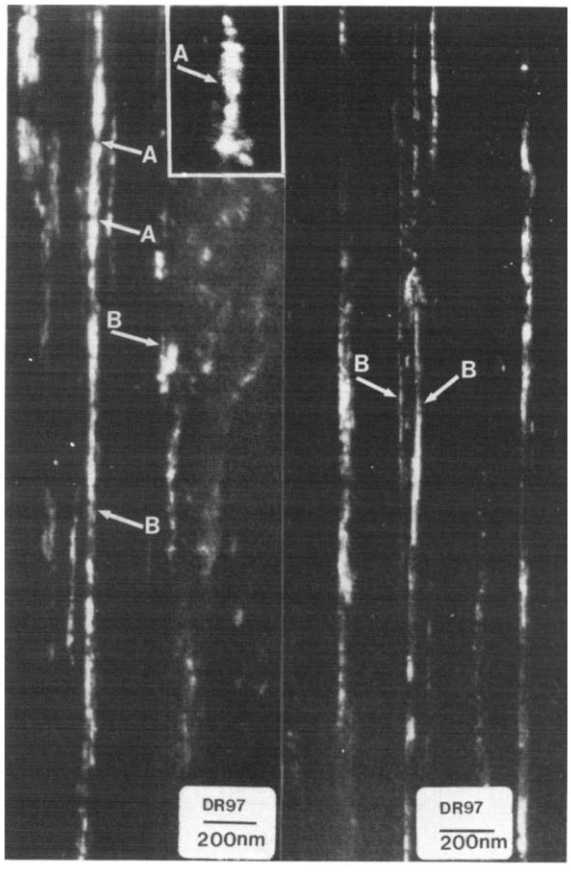

Figure 6 Darkfield micrograph of SSE/PD UHMWPE, draw ratio of 97, showing long crystalline regions interconnected by crystalline bridges (A), and protofibrils (B)

The shish-kebab-like morphology of these protofibrils was particularly evident (*Figure 8*, region C). Moreover, protofibrils bridged discontinuities in long crystalline regions (*Figure 8*, region D). These observations were reproduced for samples not subjected to nitric acid etching. For example, *Figure 10* displayed individual protofibrils (regions A) as well as coalesced protofibrils (regions B). The overall morphology was fibrous (region C). Unfortunately, the resolution of detachment replicas from unetched samples was not as high as for the more friable, etched material.

Electron diffraction data on these samples indicated a high degree of chain axis orientation in the crystalline phase at all draw ratios (*Figure 11*). A comparison of the azimuthal arcing of equatorial reflections indicated that crystalline phase orientation with respect to the draw direction increased with draw ratio. Moreover, the peak breadth of crystalline equatorial reflections increased with increasing draw ratio, indicating that deformation brought about a reduction in the average crystallite size and/or perfection perpendicular to the chain axis. The (0, 0, 2) reflection was typically sharp at both draw ratios. (The low exposures used to enhance differences between the equatorial reflections resulted in low (0, 0, 2) reflection intensity.)

To summarize, the observations made here, coupled with the mechanical and morphological characterization data of others, strongly support the formation of a sample-spanning or near sample-spanning crystalline phase in ultradrawn (SSE/PD) single crystal mats. Unequivocal proof of the existence of a sample-spanning crystalline phase requires the use of a serial sectioning technique, rather than the surface replication technique employed here. Such an approach, however, would greatly increase the complexity of the experiment, because hardening, embedding, sectioning, and comparison of adjacent sections is then required. The much simpler detachment replication technique enabled processes which could lead to the formation of a continuous crystalline phase to be seen.

Solid state extrusion to a draw ratio of six brought about deformation of the original single crystal mats, and

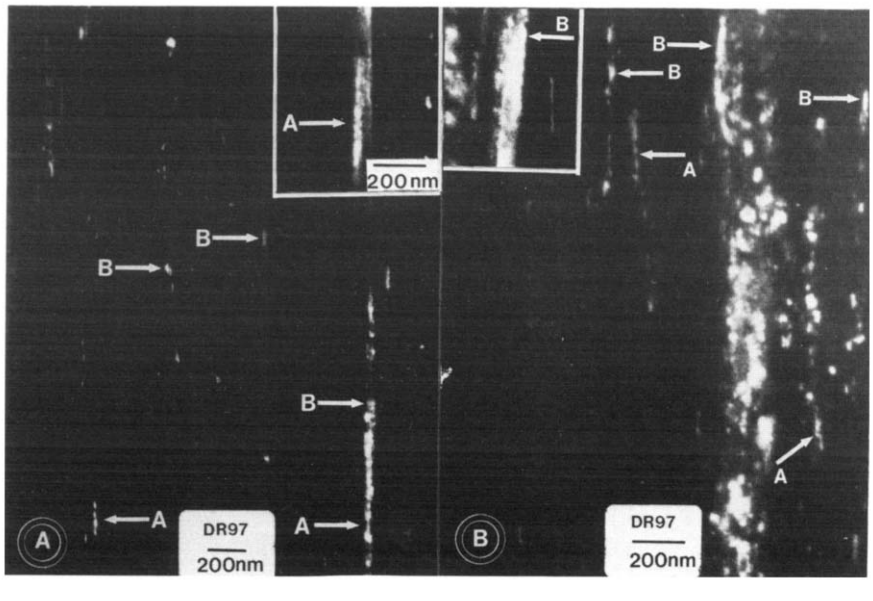

Figure 7 Darkfield micrograph of SSE/PD UHMWPE, draw ratio of 97, showing mosaic blocks being drawn into protofibrils (A), and laterally coalesced protofibrils as well as wide crystalline regions (B). The inset reveals that lamellae are still present

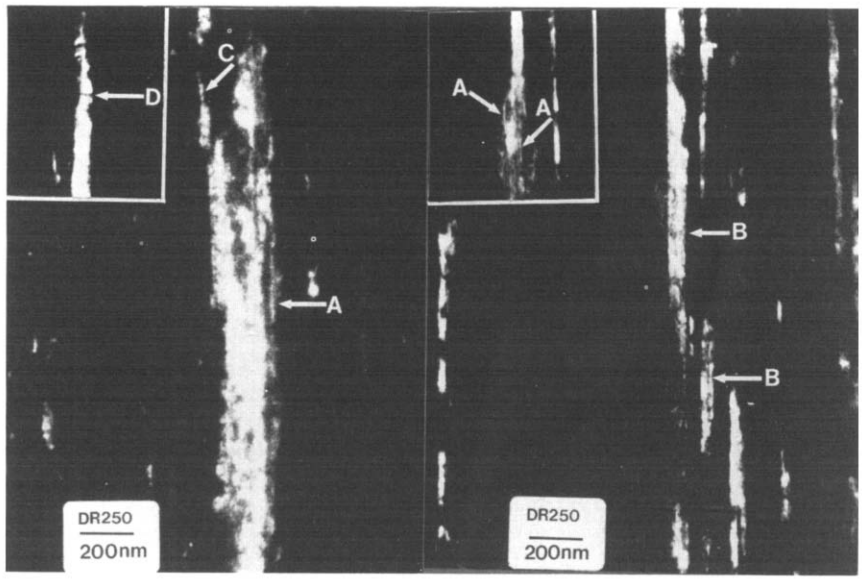

Figure 8 Darkfield micrographs of SSE/PD UHMWPE of draw ratio 250, showing protofibrils (A), large crystalline regions which appear to be composed of protofibrils (B), shish-kebab-like protofibrils (C), and protofibrils interconnecting large crystalline regions (D)

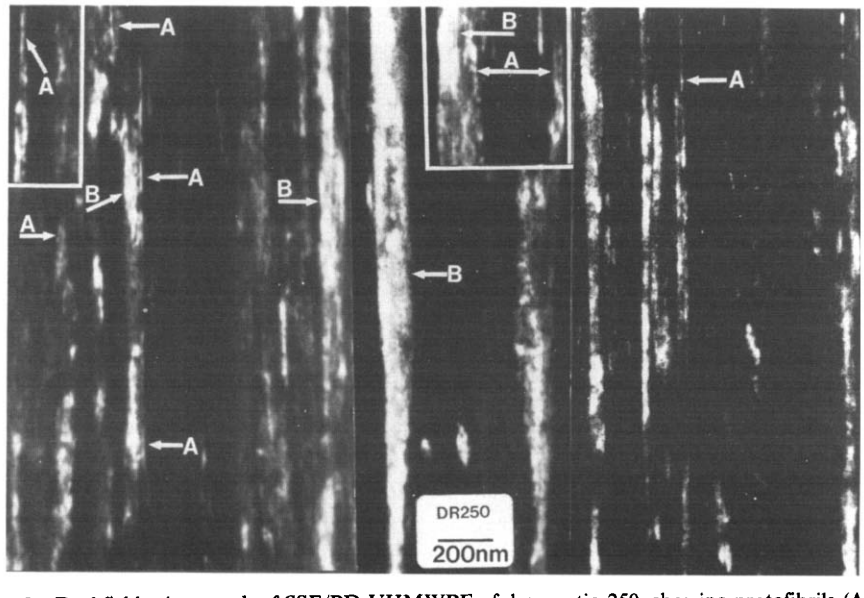

Figure 9 Darkfield micrograph of SSE/PD UHMWPE of draw ratio 250, showing protofibrils (A) and large crystalline regions composed of protofibrils (B)

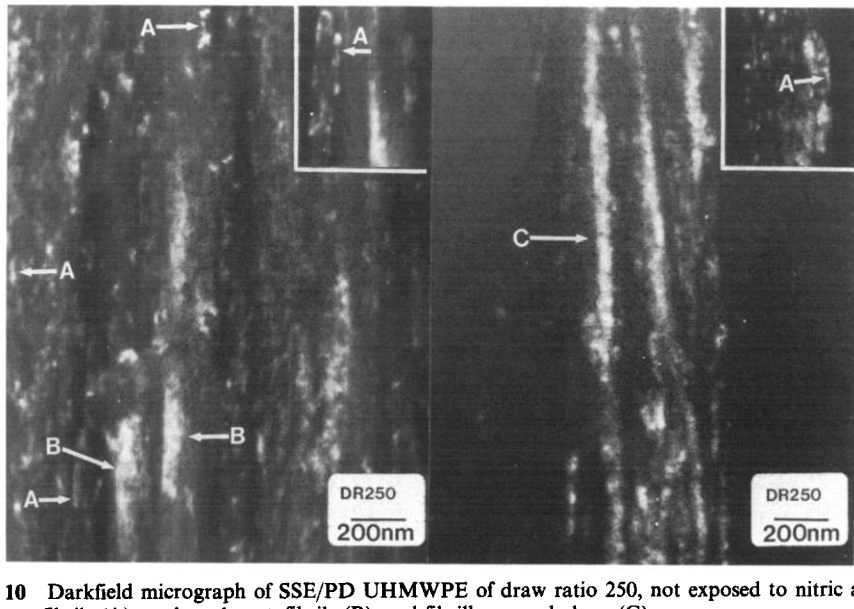

Figure 10 Darkfield micrograph of SSE/PD UHMWPE of draw ratio 250, not exposed to nitric acid. Note protofibrils (A), coalesced protofibrils (B), and fibrillar morphology (C)

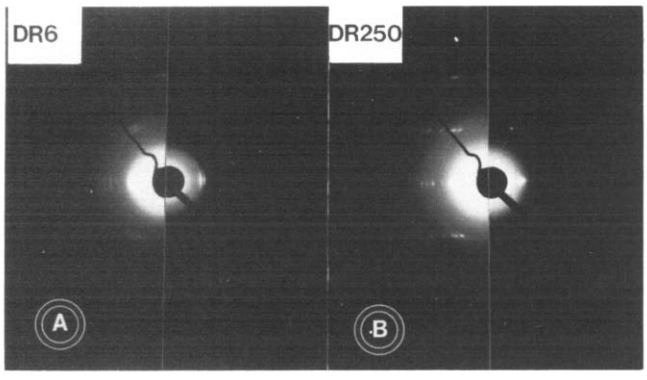

Figure 11 Electron diffraction patterns taken with beam perpendicular to chain axis of UHMWPE solid state extruded to (a) a draw ratio of 6, and (b) a draw ratio of 250. Each diffraction pattern is shown at two different printing exposures

strain-induced crystallization of (extended and highly oriented) chains. This transformed the initial single crystal morphology to one composed of stacked lamellae. Such a morphology is well represented by the structural model of Gibson *et al.*[30] in which lamellae are stacked within microfibrils and are interconnected by crystalline bridges.

At higher draw ratios, the periodic alternation of chain-folded crystals and amorphous phase gave way to the highly crystalline protofibril morphology. At a draw ratio of 42, protofibrils coexisted with chain-folded lamellae and mosaic blocks, whereas the morphology of material drawn to a draw ratio of 250 was dominated by a protofibril substructure. This explained the known reduction in SAXS long period peak intensity and eventual total disappearance of the peak with draw. The concomitant occurrence of crystallite deformation and strain-induced (re)crystallization can be used to explain the variation of sample density and crystal thickness with draw. The reduction in density at low extrusion draw ratio most likely corresponded to a loss of crystallinity and crystal perfection during deformation (assuming cavitation to be minimized by the hydrostatic pressure accompanying SSE).

The combined use of SSE and PD led to a high degree of chain extension, an increase in crystallinity, and ultimately to an ultrahigh tensile modulus material with a morphology of laterally coalesced protofibrils. The high modulus and strength of these ultradrawn materials indicates that the protofibrils reinforce these ultradrawn films to a great extent, the mechanical properties approaching those expected for a continuous crystalline phase.

CONCLUSIONS

The evolution of morphology with draw was shown for ultrahigh molecular weight polyethylene single crystal mats which were solid state extruded to a draw ratio of 6 and post-drawn to draw ratios as high as 250 at elevated temperatures. The ultradrawn samples have previously been shown to exhibit tensile moduli of 175 GPa and strengths of 3 GPa at room temperature, as well as weight average crystallinities of ca. 90%. Crystalline regions as extensive as 3 microns (along the chain direction) were observed at high draw ratios by darkfield TEM. Since darkfield microscopy gives only a lower bound of crystal size, the crystals present may be even longer. Indeed, both mechanical and morphological data strongly suggest the formation of a continuous crystalline phase in ultra-drawn polyethylene.

Protofibrils, the elementary fibrillar units found by darkfield microscopy, were typically hundreds of nanometres long and consisted of a series arrangement of ca. 8 nm thick crystalline blocks interconnected by crystalline bridges. They can be easily differentiated from microfibrils in that they do not display well defined alternating crystalline and amorphous phases. Rather, protofibrils appear structurally similar to needle crystals. Protofibrils formed by a stress-induced transformation of the crystalline phase. The deformation process was likened to that observed previously in thin films[27]. Lamellae were reduced to their mosaic block components, which sheared apart along the ⟨001⟩ direction. Moreover, mosaic block thickness was reduced to less than 10 nm by the generation of defective regions within thicker (20 nm) crystalline blocks. These smaller blocks then fed into the protofibrils. The strain-induced crystallization processes which accompanied the transformation of the single crystal to stacked lamellar morphology by a draw ratio of 6, are believed equivalent to those which led to protofibril formation at still higher draw ratios.

To conclude, the crystalline bridge model of Gibson *et al.*[30] is a good representation of material drawn to a draw ratio of ca. 6, but is not applicable to ultradrawn material where a long period is no longer observable by TEM. Instead, ultradrawn material can be represented by a model consisting of the lateral coalescence of protofibrils. This is consistent with the known fibrous nature of ultradrawn material.

ACKNOWLEDGEMENTS

We would like to thank Dr T. Kanamoto, Science University of Tokyo, for supplying drawn polyethylene samples. We also thank the Materials Research Laboratory, University of Massachusetts, for the use of their facilities, and gratefully acknowledge the support of the National Science Foundation, Grant DMR84-06079 (Polymers Program).

REFERENCES

1 Perkins, W. and Porter, R. S. *J. Materials Sci.* 1977, **12**, 2355
2 Zachariades, A. E., Mead, W. T. and Porter, R. S. *Chem. Rev.* 1980, **80**, 351
3 Chuah, H. H., De Micheli, R. and Porter, R. S. *J. Polym. Sci., Lett.* 1983, **21**, 791
4 Kanamoto, T., Tsuruta, A., Tanaka, K., Takeda, M. and Porter, R. S. *Rep. Prog. Polym. Phys., Japan* 1983, **26**, 347
5 Irvine, P. A. and Smith, P. *Macromolecules* 1986, **19**, 240
6 Ito, M., Kanamoto, T., Tanaka, K. and Porter, R. S. *Macromolecules* 1981, **14**, 1779
7 Gibson, A. G., Ward, I. M., Cole, B. N. and Parsons, B. *J. Mater. Sci.* 1974, **9**, 1193
8 Kanamoto, T., Tsuruta, A., Tanaka, K., Takeda, M. and Porter, R. S. *Polym. J.* 1983, **15**, 327
9 Furuhata, K., Yokokawa, T., Seoul, C. and Miyasaka, K. *J. Polym. Sci., Phys. Edn.* 1986, **24**, 59
10 Kanamoto, T., Fujimatsu, S., Tsuruta, A., Tanaka, K. and Porter, R. S. *Rep. Prog. Polym. Phys., Japan* 1981, **24**, 185
11 Tsuruta, A., Kanamoto, M., Tanaka, K. and Porter, R. S. *J. Polym. Sci., Phys. Edn.* 1985, **23**, 429
12 Adams, W. W., Briber, R. M., Sherman, E. S., Porter, R. S. and Thomas, E. L. *Polymer* 1985, **26**, 17
13 Peterlin, A. *Polym. Eng. Sci.* 1976, **16**, 126

14 Adams, W. W., Yang, D. and Thomas, E. L. *J. Materials Sci.* 1986, **21**, 2239
15 Kanamoto, T., Ito, M., Ogura, K., Tanaka, K. and Porter, R. S. 'Polymers For Fibers and Elastomers' (Ed. J. C. Arthur, Jr.), *ACS Symposium Series 260*, 1984, **25**, 397
16 Peterlin, A. *J. Mater. Sci.* 1971, **6**, 490
17 Sherman, E. S., Porter, R. S. and Thomas, E. L. *Polymer* 1982, **23**, 1069
18 Smith, P. J., Boudet, A. and Chanzy, H. *J. Mater. Sci. Lett.* 1985, **4**, 13
19 Frye, C. J., Ward, I. M., Dobb, M. G. and Johnson, D. J. *Polymer* 1979, **20**, 1310
20 van Hutten, P. F., Koning, C. E. and Pennings, A. J. *J. Mater. Sci.* 1985, **20**, 1556
21 Staudinger, H. 'Die Hochmolelcuren Organischen Verbindungen', Springer, Berlin, 1932
22 Hess, K. and Kiessig, H. *Naturwissenschaften* 1943, **31**, 171
23 Kanamoto, T. private communication
24 Wang, J., Harrison, I. R. *Methods of Experimental Physics* 1980, **16B**, 128
25 Kanamoto, T., Sherman, E. S. and Porter, R. S. *Polym. J.* 1979, **11**, 497
26 Zachariades, A. E. and Porter, R. S. *J. Macromol. Sci., Phys.* 1981, **B19**, 377
27 Brady, J. M. and Thomas, E. L. *J. Mater. Sci.* in press
28 Gohil, R. M. and Petermann, J. *J. Polym. Sci., Phys. Edn.* 1979, **17**, 525
29 Grubb, D. T. and Keller, A. *Colloid Polym. Sci.* 1978, **256**, 218
30 Gibson, A. G., Davies, G. R. and Ward, I. M. *Polymer* 1978, **19**, 683
31 Capaccio, G., Gibson, A. G., Ward, I. M. in 'Ultra-High Modulus Polymers' (Eds. A. Ciferri and I. M. Ward), Applied Science, London 1979, p. 1